International Journal of Electrical, Electronic and Communication Sciences
ISSN: 2517-9438
Vol:12, No:3, 2018

Spin-Dependent Transport Signatures of Bound States: From Finger to Top Gates

Yun-Hsuan Yu, Chi-Shung Tang, Nzar Rauf Abdullah, Vidar Gudmundsson

***Abstract*—**Spin-orbit gap feature in energy dispersion of one-dimensional devices is revealed via strong spin-orbit interaction (SOI) effects under Zeeman field. We describe the utilization of a finger-gate or a top-gate to control the spin-dependent transport characteristics in the SOI-Zeeman influenced split-gate devices by means of a generalized spin-mixed propagation matrix method. For the finger-gate system, we find a bound state in continuum for incident electrons within the ultra-low energy regime. For the top-gate system, we observe more bound-state features in conductance associated with the formation of spin-associated hole-like or electron-like quasi-bound states around band thresholds, as well as hole bound states around the reverse point of the energy dispersion. We demonstrate that the spin-dependent transport behavior of a top-gate system is similar to that of a finger-gate system only if the top-gate length is less than the effective Fermi wavelength.

***Keywords*—**Spin-orbit, Zeeman, top-gate, finger-gate, bound state.

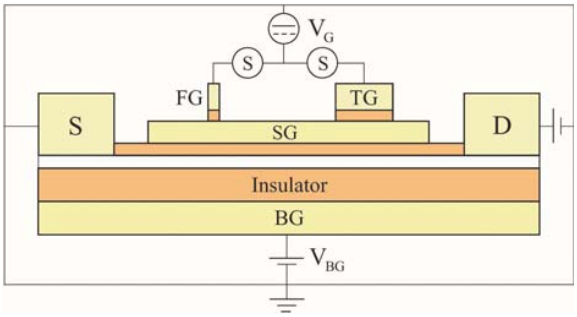

Fig. 1 Side-view of the spin transport device. A gate voltage $V_{\rm G}$ is applied to control the split-gate (SG) confined narrow constriction under a small drain-source bias. The left or right switch (S) is used to select the finger-gate (FG) or the top-gate (TG) system. These gates are electrically isolated using cross-linked PMMA insulators [15]. An additional back-gate (BG) voltage $V_{\rm BG}$ is applied to tune the electron energy

I. Introduction

QUASI-ONE-DIMENSIONAL systems in two-dimensional electron gases (2DEGs) by applying negative voltages to individual split-gates placed on the high-mobility wafer surface are widely used for applications based on quantum coherent wave and spin nature [1]-[4]. The control of spin-dependent transport is the central theme of fundamental and technological aspects that can be achieved with strong spin-orbit interaction (SOI) in narrow-band-gap semiconductors [5]-[7] for the purposes of electron-spin generation, detection, or manipulation [8]-[10].

The SOI associated transport has attracted much attention since the Datta-Das spin transistor was proposed [5]. Since Nitta and his collaborators showed that in an inverted $In_{1-x}Ga_xAs/In_{1-x}Al_xAs$ quantum well the Rashba-type SOI can be controlled by applying a top-gate voltage [11], interest in utilizing the SOI to manipulate electron spins has thus been growing. The control of SOI is both material and structure sensitive. This feature can be demonstrated utilizing all-optical spin-dynamic measurement [12] or spin-optronic devices [13]. On the other hand, the interplay between the Rashba and the Dresselhaus effects can be probed using photo-galvanic spectroscopy [14].

Yun-Hsuan Yu is with the Department of Mechanical Engineering, National United University, Miaoli, Taiwan (e-mail: yun.shyun651@nuu.edu.tw).
Chi-Shung Tang is with the Department of Mechanical Engineering, National United University, Miaoli, Taiwan (e-mail: cstang@nuu.edu.tw).
Nzar Rauf Abdullah is with the Physics Department, College of Science, University of Sulaimani, Iraq.
Vidar Gudmundsson is with the Science Institute, University of Iceland, Iceland.

Previously, we considered a spin-orbit quantum channel influenced by an in-plane magnetic field that is controlled by a finger-gate [16], in which the evanescent modes under the gate are negligible. Later on, we have extended our calculation to a top-gate system [17], in which the evanescent modes under the gate can not be neglected. In this work, we suggest an experimental setup, shown in Fig. 1, in order to investigate the finger-gate and the top-gate systems. We assume that the physical parameters are related to the experimental studies in InAs-based quantum wells [18], [19]. In addition, a back-gate voltage is applied to tune the electron Fermi energy in the 2DEG [17].

The combination of Rashba SOI and the Zeeman field may induce a spin-split energy dispersion with symmetric spin-orbit gap [20], [21]. It was proposed that the electronic transport involving such a symmetric spin-orbit gap can be controlled via finger gates [22]-[25]. We also consider a top-gate controlled quantum device. The application of voltage at the finger-gate or the top-gate results in potential barrier in the channel and determines the shift of energy dispersion in the gate region. Consequently, we find that the electrical conductance reveals significant electron-like (hole-like) quasi-bound states (QBSs) or hole-like bound states (BSs) features. They depend on the length and voltage of the applied finger-gate or top-gate. Below we shall report our observation that the conductance behavior, involving spin-flip and spin-preserve scattering, of a top-gate system is similar to that of a finger-gate system only when the top-gate length L is approximately or less than the effective Fermi wavelength λ_F.

II. Spin-dependent Quantum Transport

In order to deal with spin-resolved transport in a spin-orbit quantum channel influenced by a finger-gate or a top-gate, we consider the two-dimensional 2×2 Hamiltonian

$$\boldsymbol{\mathcal{H}} = \boldsymbol{\mathcal{H}}_0 + \boldsymbol{\mathcal{H}}_{\rm R} + \boldsymbol{\mathcal{H}}_{\rm D} + \boldsymbol{\mathcal{H}}_{\rm Z} + U_{\rm G}(x)\mathbf{1}_{2\times 2}. \quad (1)$$

for the electron motion in a 2D plane with a gate potential energy $U_{\rm G}(x)$. The first term describes a bare quantum channel that is described by the ideal Hamiltonian $H_0 = \hbar^2 k^2/2m^* + U_{\rm SG}(y)$ containing a kinetic energy and a confining potential energy. We consider a (001) crystallographic 2DEG so that the SOI Hamiltonians can be reduced to a k-linear form $\boldsymbol{\mathcal{H}}_{\rm R} = \alpha\,(\sigma_x k_y - \sigma_y k_x)$, $\boldsymbol{\mathcal{H}}_{\rm D} = \beta(\sigma_x k_x - \sigma_y k_y)$, in which α and β are the Rashba and Dresselhaus coupling strength, respectively. The fourth term in (1) describes a Zeeman term can be expressed as $\boldsymbol{\mathcal{H}}_{\rm Z} = g\mu_B B\sigma_x$. Here $g = g_s/2$ is half of the effective gyromagnetic factor ($g_s = -15$ for InAs). The last term in (1) represents the spatial dependent gate potential energy $U_{\rm G}(x)$, that refers to either $U_{\rm FG}(x) = U_d\delta(x)$ for a finger-gate or $U_{\rm TG}(x) = U_0\theta(x)\theta(L-x)$ for a top-gate with electric potential energy $U_0 = -eV_{\rm TG}$.

In the following we employ the Fermi-level as an energy unit $E^* = E_F = \hbar^2 k_F^2/2m^*$ and the inverse wave number as a length unit $l^* = k_F^{-1}$. For simplicity, we assume the channel width $W = \pi l^* = 15.7$ nm and the ideal subband energy is simply $\varepsilon_n = n^2$. Plane wave solution for the eigenvalues gives the spin-split energy dispersion [16], [17]

$$E_n^\sigma = \varepsilon_n + k_x^2 + \sigma\sqrt{(2\beta k_x + gB)^2 + (2\alpha k_x)^2} + U_{\rm G}(x)\,. \quad (2)$$

Here, the superscript $\sigma = \pm$ indicating the spin-$\uparrow$ and spin-$\downarrow$ branches, respectively. The corresponding eigenvectors are

$$|k_x^\sigma\rangle = \frac{1}{\sqrt{2}}\begin{pmatrix} 1 \\ \sigma\exp\left[-i\arctan\left(\frac{2\alpha k_x}{gB}\right)\right] \end{pmatrix}. \quad (3)$$

In the absence of the Zeeman field ($gB = 0$) and the Dresselhaus effect ($\beta = 0$), the two laterally spin-split subbands are lowered by a spin-orbit energy and shifted in momentum by the spin-orbit wave number $k_{\rm so}^\sigma = -\sigma\alpha$ due to the Rashba effect. Moreover, the spin-orbit energy $E_{\rm so}$ (=α^2) is determined by subtraction of 'the subband bottom of the spin-$\downarrow$ branch' from 'the degenerate energy of the spin-branch crossing point' [17].

In the presence of a magnetic field ($gB \neq 0$), the spin-orbit wave number becomes

$$k_{\rm so}^\sigma(gB) = -\sigma\sqrt{\alpha^2 - \left(\frac{gB}{2\alpha}\right)^2}. \quad (4)$$

The spin-orbit energy $E_{\rm so}$ would be modified by the magnetic field, defined by the energy difference between the spin-$\downarrow$ branch top $E_{\rm top}^-(gB)$ and the spin-$\downarrow$ branch bottom $E_{\rm bottom}^-(gB)$, to be a magneto-spin-orbit energy $E_{\rm mso}$ involving a linear and a quadratic term of the Zeeman factor [17].

In order to investigate quantum transport properties, one has to take all the possible propagating and evanescent modes into account by considering an incident electron energy $E_n = E - \varepsilon_n$ that gives the quantum dynamic equation [25]

$$k_x^4 - \left[4(\alpha^2+\beta^2) + 2E_n\right]k_x^2 - 4\beta g B k_x + \left[E_n^2 - (gB)^2\right] = 0\,. \quad (5)$$

The spin-dependent propagation matrix describing the gate-controlled transport dynamics can be expressed as a 4×4 matrix that can be reduced to a generalized 2×2 matrix form

$$\begin{bmatrix} \mathbf{1} \\ \mathbf{r} \end{bmatrix} = \mathbf{P}\begin{bmatrix} \mathbf{t} \\ \mathbf{0} \end{bmatrix} = \begin{bmatrix} \mathbf{p}_{11} & \mathbf{p}_{12} \\ \mathbf{p}_{21} & \mathbf{p}_{22} \end{bmatrix}\begin{bmatrix} \mathbf{t} \\ \mathbf{0} \end{bmatrix} \quad (6)$$

where $\mathbf{p}_{ij}$ are 2×2 matrices. The transmission and reflection matrices can be easily obtained respectively using $\mathbf{t} = \mathbf{p}_{11}^{-1}$ and $\mathbf{r} = \mathbf{p}_{21}\mathbf{p}_{11}^{-1}$ involving spin-preserve (diagonal terms) and spin-flip (off-diagonal terms) scattering processes.

Employing the generalized propagating matrix method to solve the spin-dependent quasi-one-dimensional Schrödinger equation, one obtains the spin-polarized zero-temperature conductance based on the Landauer-Büttiker framework [26], [27].

$$G = g_0\sum_n\sum_{\sigma=\pm}\sum_{\sigma'=\sigma,\bar\sigma}\frac{v_n^{\sigma'}}{v_n^\sigma}\left|t_n^{\sigma\sigma'}\right|^2. \quad (7)$$

Here $g_0 = e^2/h$ stands for the conductance quantum per spin mode and n specifies the specific propagating channel. In addition, $t_n^{\sigma\sigma'}$ includes the transmission amplitudes of electron occupying the subband n incident from the σ spin state and transmitted to the $\sigma' = \sigma$ ($\bar\sigma$) spin state through spin-preserve (spin-flip) scattering.

III. Numerical Results and Discussion

In this section we present our numerical calculation under the assumption of high-mobility InAs-$In_{1-x}Ga_xAs$ semiconductor interface with an electron effective mass $m^* = 0.023m_0$ and typical electron density $n_e \sim 10^{12}$ cm^{-2} [11]. Accordingly, the energy unit is E^* = 66 meV, the length unit l^* = 5.0 nm, the magnetic field unit $B^* = 1.14$ kT, and the spin-orbit coupling parameters α and β are in units of α^* = 330 meV·nm [22]. The gate potential energy is in units of 66 meV.

Fig. 2 (a) shows the schematic illustration of spin injection scheme in a finger-gate system in real space. A finger-gate potential energy U_d is applied with strong SOI. In Fig. 2 (b), we present the schematic illustration of a top-gate applied narrow constriction with positive top-gate potential energy U_0 and strong Rashba coefficient α. We notice in passing that the sensitivity of top-gate length can not be found in the finger-gate situation. This significant difference is associated with that the scattering of propagating and evanescent modes in the finger-gate region can be neglected while these scattering modes are not negligible in the top-gate devices.

In Fig. 3, we show the conductance of a finger-gate system with strong SOI in comparison with the Zeeman effect. Within the ultra-low energy regime, applying a negative finger-gate potential energy may result in a Fano line-shape. The Fano dip (peak) is due to the quantum interference between the localized

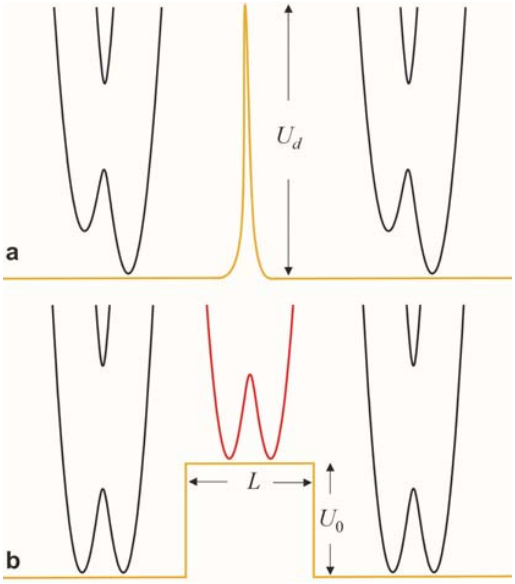

Fig. 2 Schematic of spin-split energy dispersion and spin injection scheme. (a) Dispersion relations at α = 0.2, β = 0.1, gB = 0.02 with a delta-profile finger-gate potential energy U_d. (b) Dispersion relations at α = 0.15, β = 0, gB = 0.015 with a rectangular-profile top-gate potential energy U_0 of length L

BS below the left spin-↓ branch bottom $E_{0\mathrm{L}}^{-}$ at $k_x/k_F = -0.22$ and the extended left-going (right-going) states at the right spin-↓ branch above $E_{0\mathrm{R}}^{-}$. This binding energy of the localized BS can be analytically predicted by $E_{\mathrm{FG}}^{b} = U_d^2/4$. From our numerical results, these binding energies E_{FG}^{b} are determined by $E_{0\mathrm{R}}^{-} - E_{\mathrm{FG}}^{\mathrm{BS}}$, that is, 0.0054, 0.0096, and 0.0051, for $U_d = -0.15$, -0.20, and -0.25, respectively. The mean absolute percentage error of the analytical formula $U_d^2/4$ is within 4%.

If the electron energy is within the spin-orbit gap (single-mode spin injection), the mirror effects between the hole-like and the electron-like QBSs are clearly shown. The hole-like QBS feature is found for electrons with incident energies $E_{\mathrm{FG}}^{\mathrm{HQBS}}$ = 0.9837, 0.9844, 0.9850 for U_d = 0.15, 0.20, 0.25, respectively, around E_{top}^{-}. Accordingly, the electron-like QBS feature is also found for electrons with incident energies $E_{\mathrm{FG}}^{\mathrm{EQBS}}$ = 1.0174, 1.0168, 1.0161 for $U_d = -0.15, -0.20, -0.25$, respectively, around $E_{\mathrm{bot}}^{+} = \varepsilon_1 + gB$ = 1.015.

Fig. 4 (a) shows the spin-split energy dispersion in the leads (black) and in the top-gate (color) regions. The corresponding conductance spectra are demonstrated in Figs. 4 (b)-(d). The other parameters are the same with Fig. 2 (b). Here the spin-polarized electrons are injected from the spin-orbit gap in the lead to the low-energy regime in the top-gate with spin-preserve and spin-flip intermediate forward and backward scattering.

Fig. 4 (b) shows the application of top-gate with short length L = 30 nm (less than the Fermi wavelength λ_{F}), the electron modes in the lead region dominate the transport properties. For applying a positive (negative) top-gate potential energy $U_0 = \pm 0.025$, the conductance spectrum reveals a hole-like (electron-like) QBS feature located around $E_{\mathrm{top}}^{-}(0)$ = 0.983

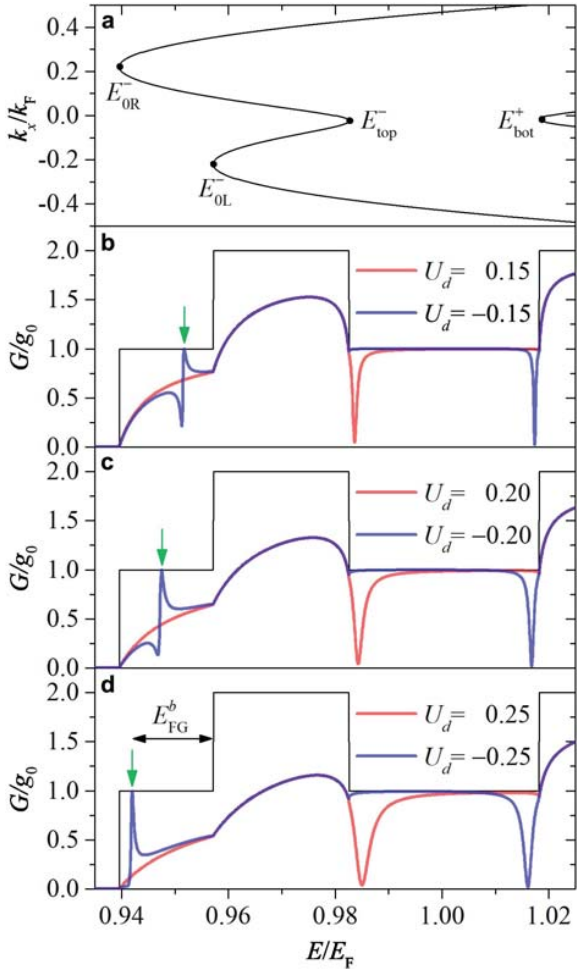

Fig. 3 Spin-split energy dispersion and finger-gate polarity dependent conductance feature with α = 0.2, β = 0.1, gB = 0.02. (a) Energy dispersion with the same parameters as Fig. 2 (a). Corresponding energy characteristics of conductance are presented for finger-gate strength U_d = (b) ±0.15, (c) ±0.20, and (d) ±0.25. The Fano line-shape in conductance is indicated by green arrow (with binding energy E_{FG}^{b}) for electrons with incident energy below $E_{0\mathrm{L}}^{-}$ in the ultra-low energy regime

($E_{\mathrm{bot}}^{+} = \varepsilon_1 + gB$ = 1.015) in the leads, respectively. We see that the prefect mirror effect between the positive and negative top-gate voltages in the finger-gate system will be partially broken in the top-gate system. The broader conductance valley of the hole-like QBS implies a shorter life time.

For an intermediate top-gate length L = 110 nm ($\simeq 3.5\lambda_{\mathrm{F}}$) shown in Fig. 4 (c), the electron occupying the outer propagating mode in the leads may be scattered to the bottom of the spin-↓ branch within the top-gate region. The electron reveals an electron-like QBS feature with energies beneath the subband bottom of the spin-↓ branch

$$E_{\mathrm{bot}}^{-}(U_0) = \varepsilon_1 - E_{\mathrm{so}} - \left(\frac{gB}{2\alpha}\right)^2 + U_0\,. \qquad (8)$$

For applying U_0 = 0.020, the conductance spectrum reveals an electron-like QBS feature located around $E_{\mathrm{bot}}^{-}(U_0)$ = 0.995. This is because the electron dwell time in the top-gate region

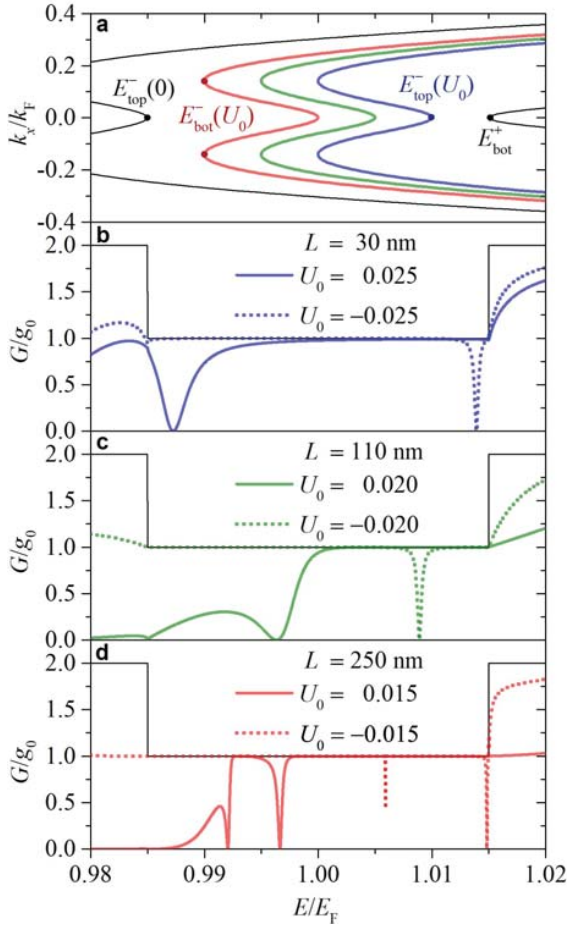

Fig. 4 Spin-split energy dispersion and top-gate polarity and length dependent conductance feature with α = 0.15, β = 0.0, gB = 0.015. (a) Energy dispersion with the same parameters as Fig. 2 (b) for U_0 = 0 (black), 0.015 (red), 0.020 (green), and 0.025 (blue). Corresponding energy characteristics of conductance are presented for (b) L = 30 nm and U_0 = $\pm$0.025; (c) L = 110 nm and U_0 = $\pm$0.020; (d) L = 250 nm and U_0 = $\pm$0.015

is enhanced, and the U_0-shifted energy dispersion becomes significantly important. On the other hand, for $U_0 = -0.020$, the conductance spectrum exhibits a red-shifted electron-like QBS feature below E^+_{bot}.

For a sufficient long top-gate length L = 250 nm ($\simeq 8\lambda_F$) shown in Fig. 4 (d), the electron dwell time in the top-gate region can be significantly enhanced and favors multiple scattering. Consequently, for applying U_0 = 0.015, the conductance spectrum reveals a hole-like BS feature for electrons with incident energy at the reverse point in the lower spin branch at the top-gate applied region. Here the electrons occupy the inner modes below the top-gate shifted lower subband top energies $E^-_{top}(U_0) = E^-_{top}(0) + U_0$, in which $E^-_{top}(0) = 0.985$ is the unshifted lower subband top. These hole-like BS energies are corresponding to the reverse point in the top-gate-shifted lower-spin branch. Furthermore, a top-gate electron-like QBS around $E^-_{bot}(U_0)$ can be also found. For applying a negative gate-potential energy $U_0 = -0.015$, the conductance spectrum exhibits a double electron-like QBS feature at energies E = 1.006 and 1.015 below the upper spin branch bottom.

IV. Conclusion

We have considered a spin-orbit quantum channel controlled by either a finger-gate or a top-gate in the presence of an external longitudinal magnetic field. The Rashba-Dresselhaus-Zeeman effect may induce an asymmetric spin-split energy spectrum, while the Rashba-Zeeman effect induces a symmetric spin-split energy spectrum.

The transport behavior of the finger-gate system is summarized as follows. In the ultra-low energy regime, bound states are found exhibiting the Fano line-shape or a simple peak depending on the strength of the negative finger-gate potential energy. In the low energy regime, the conductance is insensitive to the finger-gate voltage. In the spin-orbit gap energy regime, mirror effect between the hole-like and electron-like quasi-bound states is significantly recognized.

We have also considered a top-gate controlled quantum device with spin-orbit coupling and an external in-plane magnetic field, in which all the propagating modes with real wave vectors and the evanescent modes with complex wave numbers in the gate region have to be taken into account. Since the effective spin-orbit field B_{so} is perpendicular to the effective Zeeman field gB, the spin-orbit gap can be significantly induced in the strong spin-orbit coupling regime. Transport signatures have been demonstrated for electrons incident from spin-orbit gap energies though a top-gate region with positive or negative electric potential energies.

Acknowledgment

The authors acknowledge financial supports from Ministry of Science and Technology in Taiwan under grant No. 106-2112-M-239-001-MY3, and the National Center for Theoretical Sciences in Taiwan.

References

[1] D. A. Wharam, T. J. Thornton, R. Newbury, M. Pepper, H. Ahmed, J. E. F. Frost, D. G. Hasko, D. C. Peacock, D. A. Ritchie, G. A. C. Jones, "One-dimensional transport and the quantisation of the ballistic resistance", *J. Phys. C: Solid State Phys.*, vol. 21, pp.209-214, 1988.

[2] B. J. van Wees, H. van Houten, C. W. J. Beenakker, J. G. Williamson, L. P. Kouwenhoven, D. van der Marel, C. T. Foxon, "Quantized Conductance of Point Contacts in a Two-Dimensional Electron Gas", *Phys. Rev. Lett.*, vol. 60, no. 9, pp.848-850, 1988.

[3] K. J. Thomas, J. T. Nicholls, M. Y. Simmons, M. Pepper, D. R. Mace, and D. A. Ritchie, "Possible Spin Polarization in a One-Dimensional Electron Gas", *Phys. Rev. Lett.*, vol. 77, no. 1, pp.135-138, 1996.

[4] J. H. Bardarson, I. Magnusdottir, G. Gudmundsdottir, C.-S. Tang, A. Manolescu, and V. Gudmundsson , "Coherent electronic transport in a multimode quantum channel with Gaussian-type scatterers", *Phys. Rev. B*, vol. 70, no. 24, 245308, 2004.

[5] S. Datta and B. Das, "Electronic analog of the electro-optic modulator", *Appl. Phys. Lett.*, vol. 56, pp.665-667, 1990.

[6] M. Governale, D. Boese, U. ZLulicke, and C. Schroll, "Filtering spin with tunnel-coupled electron wave guides", *Phys. Rev. B*, vol. 65, no. 14, 140403, 2002.

[7] A. Aharony, O. Entin-Wohlman, Y. Tokura, and S. Katsumoto, "Spin filtering by a periodic spintronic device", *Phys. Rev. B*, vol. 78, no.12, 125328, 2008.

[8] D. D. Awschalom, D. Loss, and N. Samarth, *Semiconductor Sprintronics and Quantum Computation* (Springer, Berlin, 2002).

[9] A. G. Mal'shukov, C. S. Tang, C. S. Chu, and K. A. Chao, "Spin-current generation and detection in the presence of an ac gate", *Phys. Rev. B*, vol. 68, no.23, 233307, 2003.
[10] A. G. Mal'shukov, C. S. Tang, C. S. Chu, and K. A. Chao, "Strain-induced coupling of spin current to nanomechanical oscillations", *Phys. Rev. Lett.*, vol. 95, no. 10, 107203, 2005.
[11] J. Nitta, T. Akazaki, H. Takayanagi, and T. Enoki, "Gate Control of Spin-Orbit Interaction in an Inverted $In_{0.53}Ga_{0.47}/In_{0.52}Al_{0.48}As$ Heterostructure", *Phys. Rev. Lett.*, vol. 78, no. 7, pp.1335-1338, 1997.
[12] P. S. Eldridge, W. J. H. Leyland, P. G. Lagoudakis, O. Z. Karimov, M. Henini, D. Taylor, R. T. Phillips, and R. T. Harley, "All-optical measurement of Rashba coefficient in quantum wells", *Phys. Rev. B*, vol. 77, no. 12, 125344, 2008.
[13] A. S. Sheremet, O. V. Kibis, A. V. Kavokin, and I. A. Shelykh, "Datta-and-Das spin transistor controlled by a high-frequency electromagnetic field", *Phys. Rev. B*, vol. 93, no. 16, 165307, 2016.
[14] S. D. Ganichev and L. E. Golub, "Interplay of Rashba/Dresselhaus spin splittings probed by photogalvanic spectroscopyVA review", *Phys. Status Solidi B*, vol. 251, pp.1801-1823, 2014.
[15] I. Zailer, J. E. F. Frost, V. Chabasseur-Molyneux, C. J. B. Ford, and M. Pepper, "Crosslinked PMMA as a highresolution negative resist for electron beam lithography and applications for physics of low-dimensional structures", *Semicond. Sci. Technol.*, vol. 11, pp. 1235-1238, 1996.
[16] C.-S. Tang, J.-A. Keng, N. R. Abdullah, V. Gudmundsson, "Spin magneto-transport in a RashbaVDresselhaus quantum channel with single and double finger gates", *Phys. Lett. A*, vol. 381, pp. 1529-1533, 2017.
[17] C.-S. Tang, Y.-H. Yu, N. R. Abdullah, V. Gudmundsson, "Transport signatures of top-gate bound states with strong RashbaVZeeman effect", *Phys. Lett. A*, vol. 381, pp. 3960-3963, 2017.
[18] S. Giglberger, L. E. Golub, V. V. Belkov, S. N. Danilov, D. Schuh, C. Gerl, F. Rohlfing, J. Stahl,W.Wegscheider, D.Weiss, W. Prettl, and S. D. Ganichev, "Rashba and Dresselhaus spin splittings in semiconductor quantum wells measured by spin photocurrents", *Phys. Rev. B*, vol. 75, no. 3, 035327, 2007.
[19] C. López-Bastidas, J. A. Maytorena, and F. Mireles, "Interplay of the Rashba and Dresselhaus spin-orbit coupling in the optical spin susceptibility of 2D electron systems", *Phys. Status Solidi C*, vol. 4, pp.4229-4235, 2007.
[20] Y. V. Pershin, J. A. Nesteroff, and V. Privman, "Effect of spin-orbit interaction and in-plane magnetic field on the conductance of a quasi-one-dimensional system", *Phys. Rev. B*, vol. 69, no. 12, 121306(R), 2004.
[21] C. H. L. Quay, T. L. Hughes, J. A. Sulpizio, L. N. Pfeiffer, K.W. Baldwin, K.W.West, D. Goldhaber-Gordon, and R. de Picciotto, "Observation of a one-dimensional spinVorbit gap in a quantum wire", *Nat. Phys.*, vol. 6, pp.336-339, 2010.
[22] C.-S. Tang, S. Y. Chang, and S. J. Cheng, "Finger-gate manipulated quantum transport in a semiconductor narrow constriction with spin-orbit interactions and Zeeman effect", *Phys. Rev. B*, vol. 86, no. 12, 125321, 2012.
[23] A. F. Sadreev and E. Ya. Sherman, "Effect of gate-driven spin resonance on the conductance through a one-dimensional quantum wire", *Phys. Rev. B*, vol. 88, no. 11, 115302, 2013.
[24] D. Rainis and D. Loss, "Conductance behavior in nanowires with spin-orbit interaction: A numerical study", *Phys. Rev. B*, vol. 90, no. 23, 235415, 2014.
[25] C.-S. Tang, S.-T. Tseng, V. Gudmundsson, and S.-J. Cheng, "Double-finger-gate controlled spin-resolved resonant quantum transport in the presence of a RashbaVZeeman gap", *J. Phys. Cond. Mat.*, vol. 27, 085801, 2015.
[26] R. Landauer, "Electrical resistance of disordered one-dimensional lattices", *Philos. Mag.*, vol. 21, pp.863-867, 1970.
[27] M. Büttiker, "Quantized transmission of a saddle-point constriction", *Phys. Rev. B*, vol. 41, no. 11, pp.7906-7909, 1990.